

Optical photometry and spectroscopy of the type Ibn supernova SN 2006jc until the onset of dust formation

G. C. Anupama¹, D. K. Sahu¹, U. K. Gurugubelli^{1,2}, T. P. Prabhu¹,
N. Tominaga³, M. Tanaka^{4,5}, K. Nomoto^{5,4}

1. Indian Institute of Astrophysics, Bangalore, 560 034, India

2. Joint Astronomy Programme, Indian Institute of Science, Bangalore 560 012, India

3. Optical and Infrared Astronomy Division, National Astronomical Observatory, 2-21-1 Osawa, Mitaka, Tokyo 181-8588, Japan

4. Department of Astronomy, Graduate School of Science, University of Tokyo, Hongo 7-3-1, Bunkyo-ku, Tokyo 113-0033, Japan

5. Institute for the Physics and Mathematics of the Universe, University of Tokyo, Kashiwa, Chiba 277-8568, Japan

(E-mail: gca@iia.res.in)

Accepted.....; Received

ABSTRACT

We present optical *UBVRI* photometric and spectroscopic data of the type Ibn supernova SN 2006jc, until the onset of the dust forming phase. The optical spectrum shows a blue continuum and is dominated by the presence of moderately narrow (velocity ~ 2500 km s⁻¹) He I emission lines superimposed over a relatively weak supernova spectrum. The helium lines are produced in a pre-existing He rich circumstellar shell. The observed helium line fluxes indicate the circumstellar shell is dense, with a density of $\sim 10^9 - 10^{10}$ cm⁻³. The helium mass in this shell is estimated to be $\lesssim 0.07 M_{\odot}$. The optical light curves show a clear signature of dust formation, indicated by a sharp decrease in the magnitudes around day 50, accompanied by a reddening of the colours. The evolution of the optical light curves during the early phase and that of the *uv* bolometric light curve at all phases is reasonably similar to normal Ib/c supernovae.

Key words: supernovae: general - supernovae: individual: SN 2006jc - circumstellar matter

1 INTRODUCTION

Core collapse supernovae (CCSNe) signify the end of the most massive stars. They are categorized, spectroscopically, as type II, IIb, Ib and Ic by the presence of strong hydrogen, helium and weak hydrogen, helium alone and no hydrogen or helium, respectively (see Filippenko 1997 for a review). Type IIn are those objects that show narrow hydrogen emission lines as a result of the interaction of the supernova ejecta with a dense circumstellar medium (CSM) (Schlegel 1990, Chugai & Danziger 1994). Wolf-Rayet stars, i.e., massive stars that have been stripped off their outer hydrogen and/or helium layers due to mass loss during the course of their evolution, are believed to be the progenitors of the stripped-envelope CCSNe (IIb, Ib, Ic). The possibility of yet another class of stripped-envelope CCSNe emerged with the detection of moderately narrow helium emission lines in SN 1999cq (Matheson et al. 2000), similar to the presence of narrow hydrogen lines in type IIn. Matheson et al. suggested an interaction of the supernova ejecta with a dense CSM that had little or no hydrogen. SN 2002ao (Martin et al. 2002, Filippenko & Chornock 2002) was identified to be similar to SN 1999cq. The recent discovery of SN 2006jc with strong,

moderately narrow helium emission lines, and weak hydrogen lines has added to the list of this new, interesting class of CCSNe, now designated as Ibn (Pastorello et al. 2008).

Supernova SN 2006jc was discovered by K. Itagaki, at a magnitude of 13.8, on Oct 9.75 UT on an unfiltered image (Nakano et al. 2006). The non-detection of this object on an image obtained on Sep 22 suggests the supernova was discovered shortly after explosion. Based on the presence of strong helium features in the early spectra, the event was classified to be of type Ib (Fesen et al. 2006, Crots et al. 2006). The similarity of SN 2006jc with SNe 1999cq and 2002ao was first noted by Benetti et al. (2006).

The progenitor of this supernova is believed to have experienced a luminous outburst, similar to those of luminous blue variables (LBVs) two years prior to the supernova event (Nakano et al. 2006, Pastorello et al. 2007). Multiwavelength observations of this supernova have shown it to be unique in many respects. Early *Swift* UVOT observations on 2006 October 13 by Brown et al. (2006) indicate extremely blue UV-V colours. X-ray emission has also been observed by the *Swift* (X-Ray Telescope) and the *Chandra* satellites (Immler et al. 2008). On the contrary, SN 2006jc was not detected in the early-time radio observation (Soderberg 2006). The

X-ray emission and the UV excess are attributed to an interaction of the supernova ejecta with a shell of material deposited during the recent luminous outburst of the progenitor (Immler et al. 2008).

The optical spectra (Pastorello et al. 2007, Foley et al. 2007) show a prominent blue continuum that lasts well into the onset of the nebular phase. Around 75 days since maximum, the steepness of the blue continuum had dropped, while the continuum in the red had brightened, with the overall spectrum taking a "U"-shape (Smith et al. 2008). The red excess had disappeared by day 128. Interestingly, the optical light curves showed a sharp decline after day 50, while the near infrared luminosities brightened during the same epoch (Arkharov et al. 2006, Minezaki et al. 2007; Smith et al. 2008). The NIR excess peaked around 80 days and persisted to past 200 days (Di Carlo et al. 2008, Mattila et al. 2008; Sakon et al. 2007). Smith et al., Di Carlo et al, and Mattila et al., attribute this NIR excess to the formation of a hot dust in an outward shock-formed cool dense shell, while Sakon et al. (2008), Nozawa et al. (2008) and Tominaga et al. (2008) propose dust formation in the supernova ejecta.

We present in this paper the optical photometric and spectroscopic observations of SN 2006jc obtained with the 2m Himalayan Chandra Telescope during 2006 October 14 – 2007 January 13.

2 OBSERVATIONS

Photometric monitoring of SN 2006jc in the *UBVR* and *I* bands began on 2006 October 16 (JD 2454025.45) and continued until 2007 January 13 (JD 2454114.40), using the Himalaya Faint Object Spectrograph Camera (HFOSC). Photometric standard fields (Landolt 1992) PG0231+051 and PG0942-029 were observed on 2006 November 23 and the fields PG1047+003, PG0942-029 and PG1323-086 were observed on 2006 December 27 under photometric conditions. These were used to calibrate a sequence of secondary standards in the supernova field. The data reduction and photometry was done in the standard manner, using the various tasks available within IRAF. The observed data were bias subtracted, flat-field corrected and cosmic-ray hits removed. Aperture photometry was performed on the standard stars, using an aperture radius determined using the aperture growth curve, and were calibrated using the average colour terms and photometric zero points determined on the individual nights. The *UBVRI* magnitudes of the secondary standards in the supernova field, calibrated and averaged over the two nights are listed in Table 1. The secondary sequence is shown in Figure 1, marked by numbers. The magnitudes of the supernova and the local standards were estimated using the profile fitting technique, using a fitting radius equal to the FWHM of the stellar profile. The difference between the aperture and profile-fitting magnitude (aperture correction) was obtained using the bright standards in the supernova field and this correction was applied to the supernova magnitude. The calibration of the supernova magnitude to the standard system was done differentially with respect to the local standards.

Spectroscopic monitoring of SN 2006jc began on 2006 October 14 (JD 2454023.47) and continued until 2006 Dec

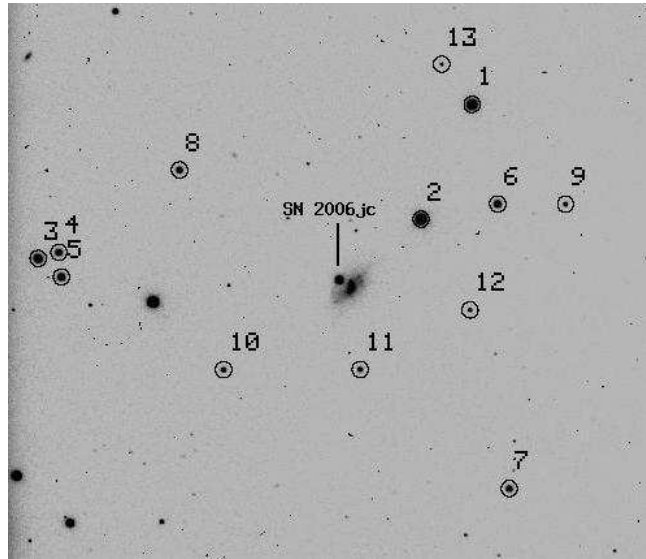


Figure 1. The field of SN 2006jc. Stars used as secondary standards and listed in Table 1 are marked.

Table 2. Log of spectroscopic observations of SN 2006jc

Date	J.D. 2450000+	Phase* (days)	ResIn Å	Range Å
2006 Oct 14	4023.47	7.5	7	3500-7800; 5200-9250
2006 Oct 16	4025.49	9.5	7	3500-7800; 5200-9250
2006 Oct 17	4026.44	10.5	7	3500-7800; 5200-9250
2006 Oct 20	4029.49	13.5	7	3500-7800; 5200-9250
2006 Oct 23	4032.46	16.5	7	3500-7800; 5200-9250
2006 Oct 24	4033.43	17.5	7	3500-7800; 5200-9250
2006 Oct 29	4038.45	22.5	7	3500-7800; 5200-9250
2006 Oct 30	4039.48	23.5	7	3500-7800; 5200-9250
2006 Nov 01	4041.48	25.5	7	3500-7800; 5200-9250
2006 Nov 05	4045.37	29.4	7	3500-7800; 5200-9250
2006 Nov 07	4047.42	31.4	7	3500-7800; 5200-9250
2006 Nov 14	4054.45	37.5	9	3500-7800
2006 Nov 16	4055.51	39.5	7	3500-7800; 5200-9250
2006 Nov 18	4058.41	42.4	7	3500-7800; 5200-9250
2006 Nov 23	4063.34	47.3	7	3500-7800; 5200-9250
2006 Dec 14	4084.35	68.4	9	3500-7800

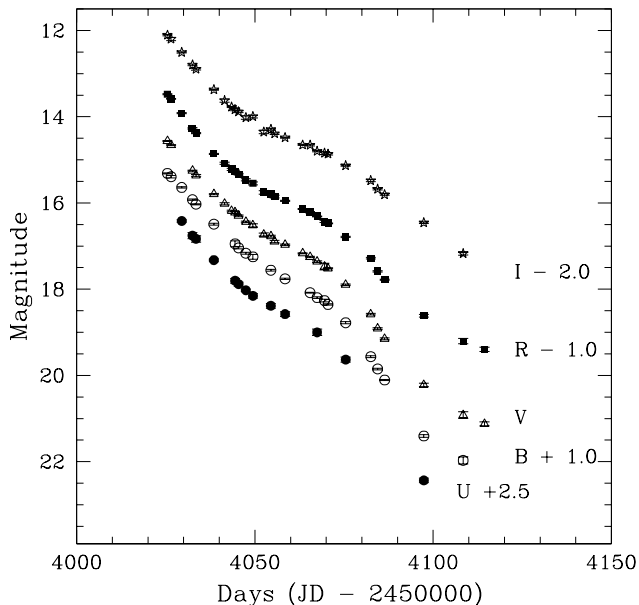
* With respect to date of maximum, assumed to be JD 2454016 (Pastorello et al. 2007)

14 (JD 2454084.35). The log of spectroscopic observations is given in Table 2. The data reduction was carried out in the standard manner using the tasks available within IRAF. The data were bias corrected, flat-fielded and the one dimensional spectra extracted using the optimal extraction method. Spectra of FeAr and FeNe lamps were used for wavelength calibration. The instrumental response curves were obtained using spectrophotometric standards observed on the same night and the supernova spectra were brought to a relative flux scale. The flux calibrated spectra in the two regions were combined to a weighted mean to give the final spectrum on a relative flux scale. The spectra were brought to an absolute flux scale using zero points derived by comparing the observed flux in the spectra with the flux estimated using the photometric magnitudes.

Table 1. Magnitudes for the sequence of secondary standard stars in the field of SN 2006jc. The stars are identified in Fig. 1.

ID	U	B	V	R	I
1	13.636 ± 0.020	13.482 ± 0.005	12.884 ± 0.010	12.537 ± 0.031	12.156 ± 0.015
2	13.005 ± 0.020	13.167 ± 0.005	12.795 ± 0.011	12.528 ± 0.020	12.202 ± 0.020
3	14.663 ± 0.030	14.280 ± 0.005	13.534 ± 0.013	13.175 ± 0.029	12.699 ± 0.053
4	15.511 ± 0.050	15.376 ± 0.005	14.749 ± 0.011	14.397 ± 0.006	14.030 ± 0.050
5	15.084 ± 0.030	14.966 ± 0.005	14.307 ± 0.010	13.937 ± 0.008	13.543 ± 0.004
6	15.142 ± 0.030	15.100 ± 0.011	14.503 ± 0.005	14.102 ± 0.003	13.722 ± 0.010
7	16.140 ± 0.037	15.742 ± 0.012	14.994 ± 0.005	14.553 ± 0.005	14.145 ± 0.005
8	16.068 ± 0.033	15.614 ± 0.005	14.739 ± 0.008	14.246 ± 0.003	13.754 ± 0.013
9	17.974 ± 0.041	17.163 ± 0.020	16.240 ± 0.006	15.712 ± 0.005	15.277 ± 0.014
10	16.862 ± 0.046	16.695 ± 0.010	16.055 ± 0.005	15.661 ± 0.005	15.255 ± 0.006
11	16.590 ± 0.032	16.705 ± 0.016	16.207 ± 0.005	15.860 ± 0.005	15.519 ± 0.015
12	18.332 ± 0.058	17.462 ± 0.013	16.545 ± 0.016	16.005 ± 0.007	15.549 ± 0.031
13	19.724 ± 0.070	18.189 ± 0.008	16.912 ± 0.023	16.127 ± 0.007	15.472 ± 0.028

The errors quoted are the statistical errors associated with the magnitudes.

**Figure 2.** *UBVRI* light curves of SN 2006jc obtained with the HCT.

3 RESULTS

3.1 Light curves

The *UBVRI* magnitudes of SN 2006jc are tabulated in Table 3 and plotted in Figure 2. Figure 3 shows the light curves of SN 2006jc compared with the light curves of a few SNe Ib/c, namely, SN 1999ex (Ib/c) ($JD_{\max,B} = 245\,1498.1$; Stritzinger et al. 2002), SN 1994I (Ic) ($JD_{\max,B} = 244\,9450.56$; Richmond et al. 1996), SN 1990I (Ib) ($JD_{\max} = 244\,8010$; Elmhamdi et al. 2004) and SN 1990B (Ic) ($JD_{\max,B} = 244\,7909.0$; Clocchiatti et al. 2001), and the type IIIn SN 1998S ($JD_{\max,R} = 245\,0890.0$; Fassia et al. 2000). The early decline ($\sim 10 - 25$ days; $JD(\max)=2454016^1$; Pastorello et al. 2007) in the *U* and *B*

bands is similar to SN 1999ex, while the decline is very similar to SN 1994I in the *VRI* bands. The *R* band light curve of SN 2006jc shows a decline during days $\sim 10 - 20$ which is slower compared with that of the type Ibn SN 1999cq (Matheson et al. 2000). Between days 30–50, a flattening is seen in all the bands, and the decline rate appears very similar to SN 1990B and SN 1990I. However, beyond day 50, SN 2006jc behaves in a quite different manner compared to the other SNe. A sharp decline is seen in all the bands, with the decline being the steepest in the *U* and *B* bands.

The *U - B*, *B - V*, *V - R* and *V - I* colours of SN 2006jc, reddening corrected using $E(B - V) = 0.05$ (Pastorello et al. 2007) are shown in Figure 4. Also shown in the Figure are the colours for SN 1999ex, SN 1994I, SN 1990I, SN 1990B and SN 1998S reddening corrected using $E(B - V)$ values 0.30 (Stritzinger et al. 2002), 0.45 (Richmond et al. 1996), 0.13 (Elmhamdi et al. 2004), 0.85 (Clocchiatti et al. 2001) and 0.22 (Fassia et al. 2000), respectively. The *U - B*, *B - V*, *V - R* and *V - I* colour curves show very little colour evolution until \sim day 60. SN 2006jc had significantly bluer *U - B*, *B - V* and *V - R* colours compared to other supernovae, while the *V - I* colour is similar to other SNe. A dramatic change in all the colours is seen beyond day 60. SN 2006jc begins to get redder, by ~ 0.5 mag. Maximum change is seen in *V - I* colour, which changes by almost 1 mag by day 100. The reddening of colours observed in SN 2006jc at later phases is not seen in other SNe, except in the case of the IIIn SN 1998S.

The sudden decline in the *UBVRI* light curves, coincident with the increase in the luminosities in the near-IR region (Arkharov et al. 2006), with a reddening of the colours are quite similar to the behaviour of dust forming novae (e.g. Gehrz 1988) and a clear indication of the formation of hot dust.

The optical ‘quasi-bolometric’ light curve is constructed using the *UBVRI* magnitudes presented here, and those published by Pastorello et al. (2007). Assuming a distance

discovered ~ 10 days after maximum light, estimated to have occurred on $JD\,2450008 \pm 15$. Since the uncertainty in the estimated epoch of maximum is quite large, we choose to follow the epoch estimated by Pastorello et al. (2007).

¹ Comparing the early spectra of SN 2006jc with those of the type Ibn SN 2000er, Pastorello et al. (2008) suggest that SN 2006jc was

Table 3. Photometric observations of SN 2006jc

Date	J.D. 2450000+	Phase* (days)	U	B	V	R	I
2006 Oct 16	4025.45	9.45		14.314 ± 0.014	14.563 ± 0.011	14.480 ± 0.013	14.107 ± 0.015
2006 Oct 17	4026.49	10.49		14.392 ± 0.026	14.659 ± 0.013	14.587 ± 0.010	14.200 ± 0.037
2006 Oct 20	4029.46	13.46	13.918 ± 0.027	14.641 ± 0.015		14.918 ± 0.013	14.508 ± 0.015
2006 Oct 23	4032.48	16.48	14.256 ± 0.070	14.925 ± 0.016	15.252 ± 0.011	15.271 ± 0.017	14.799 ± 0.018
2006 Oct 24	4033.48	17.48	14.333 ± 0.074	15.030 ± 0.012	15.360 ± 0.023	15.379 ± 0.012	14.897 ± 0.022
2006 Oct 29	4038.49	22.49	14.824 ± 0.025	15.493 ± 0.020	15.794 ± 0.013	15.864 ± 0.012	15.373 ± 0.015
2006 Nov 01	4041.49	25.49			16.018 ± 0.023	16.079 ± 0.026	15.626 ± 0.036
2006 Nov 03	4043.46	27.46			16.187 ± 0.017	16.220 ± 0.026	15.774 ± 0.014
2006 Nov 04	4044.44	28.44	15.304 ± 0.056	15.947 ± 0.069	16.218 ± 0.026	16.265 ± 0.025	15.836 ± 0.026
2006 Nov 05	4045.41	29.41	15.381 ± 0.047	16.041 ± 0.025	16.294 ± 0.017	16.334 ± 0.019	15.883 ± 0.021
2006 Nov 07	4047.45	31.45	15.524 ± 0.028	16.167 ± 0.022	16.438 ± 0.017	16.465 ± 0.025	16.019 ± 0.038
2006 Nov 09	4049.44	33.44	15.654 ± 0.051	16.249 ± 0.055	16.520 ± 0.035	16.545 ± 0.033	15.996 ± 0.030
2006 Nov 12	4052.49	36.49			16.732 ± 0.036	16.756 ± 0.043	16.353 ± 0.040
2006 Nov 14	4054.48	38.48	15.885 ± 0.055	16.559 ± 0.021	16.771 ± 0.020	16.794 ± 0.017	16.295 ± 0.017
2006 Nov 15	4055.52	39.52			16.894 ± 0.025	16.853 ± 0.029	16.392 ± 0.020
2006 Nov 18	4058.46	42.46	16.078 ± 0.053	16.760 ± 0.017	16.969 ± 0.015	16.950 ± 0.011	16.484 ± 0.013
2006 Nov 23	4063.38	47.38			17.168 ± 0.010	17.140 ± 0.010	16.655 ± 0.013
2006 Nov 25	4065.47	49.47		17.079 ± 0.010	17.254 ± 0.016	17.214 ± 0.014	16.658 ± 0.017
2006 Nov 27	4067.44	51.44	18.472 ± 0.074	17.195 ± 0.019	17.360 ± 0.017	17.312 ± 0.011	16.800 ± 0.015
2006 Nov 29	4069.51	53.51		17.263 ± 0.029	17.474 ± 0.078	17.429 ± 0.025	16.844 ± 0.031
2006 Nov 30	4070.50	54.50		17.355 ± 0.015	17.517 ± 0.012	17.473 ± 0.011	16.865 ± 0.024
2006 Dec 05	4075.45	59.45	17.132 ± 0.061	17.777 ± 0.024	17.898 ± 0.016	17.788 ± 0.013	17.133 ± 0.017
2006 Dec 12	4082.49	66.49		18.565 ± 0.021	18.580 ± 0.020	18.281 ± 0.019	17.482 ± 0.026
2006 Dec 14	4084.42	68.42		18.850 ± 0.019	18.912 ± 0.021	18.587 ± 0.014	17.680 ± 0.017
2006 Dec 16	4086.39	70.39		19.106 ± 0.014	19.150 ± 0.020	18.780 ± 0.014	17.805 ± 0.019
2006 Dec 27	4097.38	81.38	19.935 ± 0.052	20.404 ± 0.033	20.220 ± 0.039	19.617 ± 0.030	18.458 ± 0.021
2007 Jan 07	4108.42	92.42		20.971 ± 0.082	20.920 ± 0.077	20.202 ± 0.064	19.173 ± 0.036
2007 Jan 13	4114.40	98.40			21.122 ± 0.046	20.394 ± 0.050	

* With respect to date of maximum, assumed to be JD 2454016.

The errors quoted are the statistical errors associated with the magnitudes.

of 25.8 Mpc and a reddening of $E(B - V) = 0.05$ (Pastorello et al. 2007), the observed UBVRI magnitudes were converted to monochromatic fluxes and integrated over the observed wavelength range to obtain the optical quasi-bolometric light curve. Likewise, combining the NIR magnitudes (Arkharov et al. 2006, Di Carlo et al. 2007, Mattila et al. 2008) with the UBVRI magnitudes, the optical+NIR (*uvoir*) bolometric light curve was constructed integrating over the *U* to *K* bands (see also Pastorello et al. 2007, Mattila et al. 2008, Di Carlo et al. 2008, Tominaga et al. 2008). Figure 5 shows the optical ‘quasi-bolometric’ light curve as well as the *uvoir* bolometric light curve. Also shown in the Figure are the bolometric light curves of type Ib/c SNe 1990I, 1994I and 1999ex and the type II_n SN 1998S. It is evident from the plot that SN 2006jc has a luminosity that is higher than that of other Ib/c SNe, while it is about 1.6 magnitudes fainter than the type II_n SN 1998S. The optical luminosity of SN 2006jc indicates an early decline rate of 0.092 mag day⁻¹ until ~ 30 days since maximum. A flattening is seen in the light curve during $\sim 30 - 50$ days after maximum, with the decline rate during this period being 0.047 mag day⁻¹. The onset of dust formation is marked by a sharp decline in the optical luminosity, with a decline rate of 0.084 mag day⁻¹ during $\sim 50 - 100$ days after maximum. In contrast to the optical luminosity, the *uvoir* bolometric luminosity shows a flat decline, with a decline rate of 0.026 mag day⁻¹ beyond day 35. A comparison with the bolomet-

ric light curves of other SNe indicates that the bolometric light curve decline of SN 2006jc is not too different from other normal SNe Ib/c. The early decline lies between the rapidly declining SN 1994I (0.106 mag day⁻¹) and the slower SN 1999ex (0.076 mag day⁻¹), while the *uvoir* decline rate at later phases is similar to SN 1994I (0.029 mag day⁻¹).

3.2 The spectrum and its evolution

The spectrum of SN 2006jc and its evolution during the phase +7 to +68 days since the estimated maximum on JD 2454016 is presented in Figures 6 and 8. These spectra provide a fairly dense coverage of the early-time spectral evolution of SN 2006jc and are complementary in phase to those presented by Foley et al. (2007), Smith et al. (2008) and Pastorello et al. (2007, 2008). The spectrum is peculiar and different from that of normal type Ib/c supernovae (Matheson et al. 2001, Branch et al. 2002). The photospheric P Cygni profiles that are typically found in the early spectra of type Ib/c supernovae are absent, and the spectrum is characterized by (a) a steep, blue continuum shortward of ~ 5500 Å and (b) dominant moderately narrow helium emission lines.

Broad emission features, due to the expanding supernova material are also seen at $\sim 3850, 4121, 5950, 6348, 7800, 8214$ and 8500 Å. The features at $\lambda\lambda 3850, 5950, 7800$ and 8214 are identified with Mg II 3848, 3850 Å, 5938, 5943

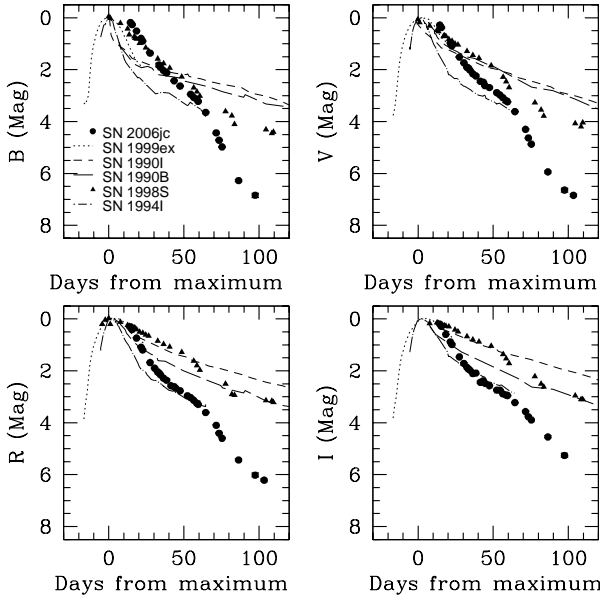


Figure 3. Comparison of the *BVRI* light curves with SNe 1999ex (Ib/c), SN 1994I (Ic), SN 1990I (Ib), SN 1990B (Ic), and SN 1998S (IIn). The magnitudes of SN 2006jc are normalized with respect to those on JD 454021.7 ($B = 14.13$, $V = 14.28$, $R = 14.18$ and $I = 13.91$; Pastorello et al. 2007), while the magnitudes of other SNe are normalized with respect to the magnitudes of their respective maximum (see text).

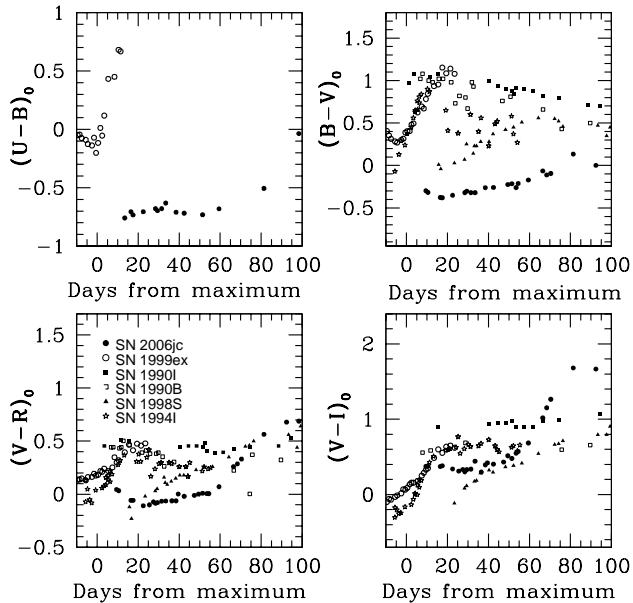


Figure 4. Reddening corrected $U - B$, $B - V$, $V - R$ and $R - I$ colour curves of SN 2006jc compared with other type Ib, Ic and IIn supernovae.

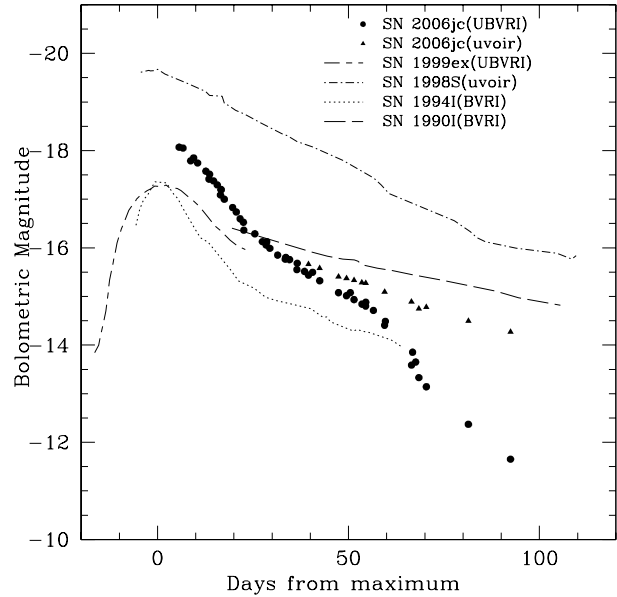


Figure 5. The optical ‘quasi-bolometric’ and the *uvoir* bolometric light curves of SN 2006jc. Also shown in the figure are the *UBVRI* bolometric light curves of the type Ib/c SN 1999ex and SN 1994I and the *uvoir* bolometric light curve of the type IIn SN 1998S.

\AA , 7790, 7877 \AA , and 8214, 8234 \AA respectively. The feature at 6348 \AA is identified with Si II λ 6355, probably blended with Mg II 6346 \AA , and the feature at 4121 \AA could be due to Si II 4128, 4131 \AA . Si II $\lambda\lambda$ 5041, 5056 could also be present. O I 7774 \AA is also present, blended with Mg II. The feature at 8500 \AA is due to Ca II infrared triplet. Mg II 4481 \AA could be blended with He I 4471 \AA . The full width at half maximum of the broad features indicate a velocity of $\sim 5000 - 6000 \text{ km s}^{-1}$. The strength of the Mg II and Si II features decrease with time, while that of the Ca II IR triplet and O I 7774 \AA increase with time. Fe II features appear to develop in the 4500-5500 \AA region, around 10 days after B maximum. The O I 7774 \AA line shows a sharp P Cygni absorption during the early phases, with the absorption minimum indicating a velocity of $\sim 620 \text{ km s}^{-1}$ (Figure 7).

The He I line widths indicate a velocity of $\sim 2200 - 3000 \text{ km s}^{-1}$. As noted by Foley et al. (2007), a narrow P Cygni component is noticed in the He I 3889 \AA line, at a velocity of $\sim 620 \text{ km s}^{-1}$. A similar component could be present in the 4471 \AA line also, at $\sim 670 \text{ km s}^{-1}$. It is interesting to note that the velocity of the narrow P Cygni absorption seen in the O I 7774 \AA line is very similar to the velocity of this component.

The line profiles of the strongest He I lines at 5876, 6678 and 7065 \AA are shown in Figure 9. From the figure, it appears that He I 5876 \AA may have a contribution from the fast moving supernova material. A broad component could be present in the 5876 \AA profile in the spectra of days 3, 5, 6 and 9. A simple de-blending of the components, assuming a simple Gaussian profile for both components, indicates the broad component has a velocity $\sim 5000 \text{ km s}^{-1}$, similar to the supernova features. The broad component fades

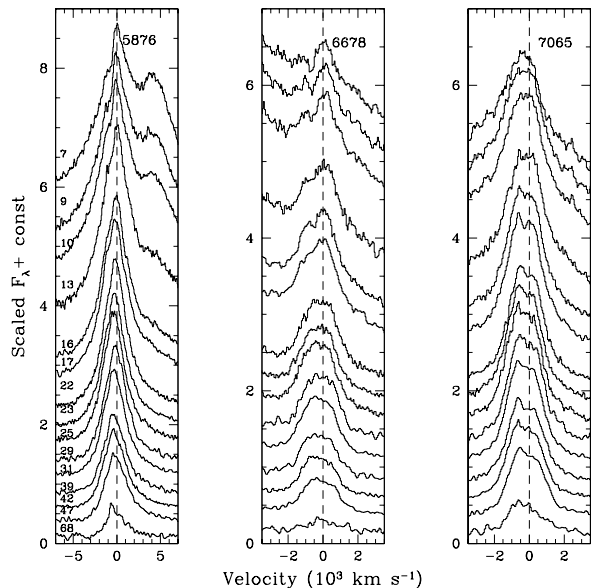


Figure 9. Evolution of the line profiles of the He I 5876, 6678 and 7065 Å lines.

and mass of the shell. The observed, reddening corrected He I 5876 Å and 7065 Å line fluxes are listed in Table 4.

If we assume the circumstellar shell (CS) ejected during the luminous mass loss episode had a velocity of 600 km s^{-1} , similar to the velocity of the narrow P Cygni absorption seen in the He I and O I lines, the radius of the shell would be $3.8 \times 10^{15} \text{ cm}$. The corresponding radius for a CS velocity of 2500 km s^{-1} , as observed for the He I emission lines is $1.6 \times 10^{16} \text{ cm}$. We also assume the thickness of the shell to be constant and determined by the observed duration (~ 10 days) of the luminous mass loss episode (Nakano et al. 2006). Using the observed reddening corrected line fluxes and a distance of 25.8 Mpc, we estimate an average density in the range $(0.54 - 3.7) \times 10^{10} \text{ cm}^{-3}$ for the shell with a velocity of 600 km s^{-1} . The corresponding mass range for this shell is $M_{\text{He}} = 0.001 - 0.008 M_{\odot}$. Likewise, for a shell velocity of 2500 km s^{-1} , the average density lies in the range $(0.6 - 4.0) \times 10^9 \text{ cm}^{-3}$ and the corresponding mass range is $M_{\text{He}} = 0.01 - 0.07 M_{\odot}$. The helium line emissivities are taken from Almgog & Netzer (1989). The density estimates are consistent with that estimated by Smith et al. (2008). Based on the observed X-ray luminosities, Immler et al. (2008) estimate a lower limit to the mass of the X-ray emitting shell to be $0.01 M_{\odot}$, and the circumstellar density to be $\sim 10^7 \text{ cm}^{-3}$. These estimates are much lower than the values implied by the helium emission lines. This indicates that the X-ray emitting region could be different from the region emitting the bulk of the helium lines.

4 DISCUSSION

SN 2006jc shows a very peculiar spectrum with a very steep blue continuum and dominated by moderately narrow He I emission lines. The presence of the moderately narrow emission lines is very similar to that observed in type II_n super-

novae, where the fast moving supernova ejecta interacts with a pre-existing circumstellar material. The observed properties of SN 2006jc are very similar to the recent supernovae SN 1999cq, SN 2000er and SN 2002ao (e.g. Pastorello et al. 2008). A weak X-ray emission and UV excess have also been detected in SN 2006jc, providing further evidence for an interaction with a pre-supernova circumstellar material (Immler et al. 2008). A luminous mass loss episode was observed in the progenitor of SN 2006jc two years prior to the outburst. It is suggested that the strong, intermediate width He I emission lines dominating the optical spectrum arise in the circumstellar shell due to the recent mass loss episode and that it is helium enriched (Foley et al. 2007, Pastorello et al. 2007, Smith et al. 2008). The fluxes of the He I emission lines indicate a density of $\sim 10^9 \text{ cm}^{-3}$ and a helium mass $\lesssim 0.07 M_{\odot}$ in the circumstellar shell that is assumed to have a velocity of 2500 km s^{-1} corresponding to the FWHM width of the He I lines. It is also quite likely that the velocity of the CSM shell was initially low, and accelerated to 2500 km s^{-1} due to the interaction. In such a case, the initial velocity of the shell is more likely to be in between the assumed velocities, and the density of the shell $\sim 10^9 - 10^{10} \text{ cm}^{-3}$. The density estimated here is similar to that estimated by Smith et al. (2008). Comparing with type II_n SNe, it is found that the estimated density range for SN 2006jc is somewhat higher than that estimated for II_n SNe, in which the CSM densities are found to range from $\sim 10^6$ (e.g. SN 1995N: Fransson et al. 2002) to $\gtrsim 10^8 \text{ cm}^{-3}$ (e.g. SN 1995G: Pastorello et al. 2002; SN 1997eg: Salamanca, Terlevich & Tenorio-Tagle 2002).

Dust formation has been observed in SN 2006jc early on, at ~ 50 days past maximum (Di Carlo et al. 2008, Smith et al. 2008, Nozawa et al. 2008). Dust formation is reflected in the helium emission line profiles, which developed an asymmetric profile, with the red wing of the profile getting increasingly suppressed with time, and also in the increase in the red to NIR continuum between 65–120 days. Smith et al. (2008) estimate the dust temperature during this phase to be $\sim 1600 \text{ K}$. The estimated densities in the shell are high enough to precipitate graphite dust (Clayton 1979).

Based on NIR and MIR observations at $t \sim 200$ days, Sakon et al. (2008) conclude that IR emission originated from amorphous carbon grains with two temperatures of 800 K and 320 K. Sakon et al., Nozawa et al. (2008) and Tominaga et al. (2008) suggest the hot carbon dust is newly formed in the supernova ejecta and heated by the ^{56}Ni – ^{56}Co decay, while the origin of the warm carbon dust is a supernova light echo of the CSM carbon dust. For the dust to originate in the SN ejecta, it implies an ejecta radius of $\sim 10^{16} \text{ cm}$ during dust formation. This in turn implies a (constant) velocity $\sim 25,000 - 30,000 \text{ km s}^{-1}$. No evidence for such a high velocity is seen in the observed spectra. Based on a comparison of the early spectra of SN 2006jc with those of SN 2000er, Pastorello et al. (2008) suggest that SN 2006jc was discovered a couple of weeks after explosion or ~ 10 days after maximum light. Very high initial velocities can thus not be ruled out, as the initial interaction of the supernova material with the CS material can lead to a deceleration of the supernova shell (e.g. Chevalier 1982).

On the basis of spectroscopic evidences, Smith et al. propose the site of dust formation to be a cold dense shell (CDS) behind the blast wave and that the shell was com-

Table 4. He I 5876 and 7065 Å emission line fluxes

Phase	Flux (10^{-14} erg cm $^{-2}$)		Density ¹ (10^9 cm $^{-3}$)		Mass ¹ (M_{\odot})	
	5876 Å	7065 Å	A ²	B ³	A ²	B ³
7.47	4.96 ⁴	9.44	16.49	1.91	0.003	0.031
9.47	7.64 ⁴	12.20	19.46	2.25	0.004	0.036
10.46	9.80 ⁴	11.59	20.48	2.36	0.004	0.038
13.48	12.28	11.12	36.27	4.18	0.008	0.066
16.45	20.24	11.68	36.86	4.24	0.008	0.070
17.44	17.52	11.35	35.24	4.07	0.008	0.066
22.46	15.79	8.70	32.17	3.71	0.007	0.059
23.49	14.48	9.51	32.23	3.71	0.007	0.059
25.49	13.65	8.48	30.83	3.55	0.007	0.057
29.37	12.27	9.30	30.89	3.55	0.007	0.057
31.42	11.29	8.08	28.97	3.34	0.007	0.055
39.51	8.59	6.82	26.14	3.01	0.005	0.049
42.42	8.49	6.25	25.43	2.94	0.005	0.048
47.35	6.95	5.45	23.43	2.70	0.004	0.043
68.36	0.758	0.725	5.41	0.63	0.001	0.011

1: Average of 5876 and 7065

2: Assuming a shell velocity of 600 km s $^{-1}$ 3: Assuming a shell velocity of 2500 km s $^{-1}$

4: Flux of de-blended narrow component

posed of dense CSM ejected by the luminous event, which was then swept up by the forward shock. They, however, do not rule out the possibility of dust formation in a carbon-rich SN ejecta. Mattila et al. (2008) also propose the CDS as the site for formation of the hot dust. However, they argue, based on the intensity, spectral energy distribution and evolution of the IR flux, that the IR emission in SN 2006jc is due to IR echoes. The bulk of the near-IR emission is due to an IR echo from the newly formed dust in the CDS, while a substantial fraction of the MIR flux is due to pre-existing dust in the progenitor wind due to an episodic mass-loss phase that ceased at least ~ 200 years before the recent pre-supernova luminous outburst and the SN event.

The observed optical light curves of SN 2006jc show an early evolution that is quite similar to normal Ib/c supernovae. The initial decline is steep and at about 20 days past maximum, the decline slows, a probable indication of the supernova having reached the exponential tail. Comparing the light curve evolution with type IIn supernovae (e.g. SN 1998S), it is seen that the early decline is much slower in the case of SNe IIn, where the light curve is thought to be powered by the interaction of the supernova material with the CSM (e.g. Rigon et al. 2003). On the other hand, the light curve evolution of SN 2006jc, until the onset of dust formation at ~ 50 days since maximum is very similar to normal Ib/c objects. Comparing the bolometric light curve of SN 2006jc with normal Ib/c SNe and the type IIn SNe, it is seen that the *uvoir* bolometric light curve of SN 2006jc is very similar to the normal Ib/c objects, with a fast early decline followed by a flattening in the light curve ~ 35 days after maximum.

It is interesting to note that while the spectrum shows clear signatures of circumstellar interaction similar to type IIn SNe, the bolometric light curve does not show any evidence of being powered by the interaction. We suggest this is possibly a result of a weaker interaction in the case of SN 2006jc due to a shell mass that is lower compared to the

mass of the circumstellar material in the case of IIn SNe (eg. $\sim 0.4 M_{\odot}$ in 1994W: Chugai et al. 2004; $\sim 10M_{\odot}$ in 1997eg: Salamanca, Terlevich & Tenorio-Tagle 2002).

5 SUMMARY

The optical spectrum and *UBVRI* light curves of SN 2006jc during the early phases, until the onset of the dust formation are presented here. The optical spectrum shows a blue continuum and is dominated by moderately narrow He I emission lines, similar to type IIn SNe and an indication of the supernova ejecta interacting with a pre-supernova circumstellar material. The moderately narrow He I emission lines arise in the pre-supernova circumstellar shell that is helium enriched.

The optical light curves show a clear signature of dust formation as indicated by a sharp decrease in the magnitudes around day 50, accompanied by a reddening of the colours. The evolution of the optical light curve during the early phases is very similar to normal Ib/c SNe. The *uvoir* bolometric light curve evolution of SN 2006jc is reasonably similar to normal Ib/c SNe at all phases.

The He I emission line fluxes indicate the circumstellar shell is dense, with a density of $\sim 10^9 - 10^{10}$ cm $^{-3}$. The helium mass in this shell is estimated to be $\lesssim 0.07 M_{\odot}$.

ACKNOWLEDGEMENTS

We thank all the observers of the 2-m HCT (operated by the Indian Institute of Astrophysics), who kindly provided part of their observing time for the supernova observations. We thank the referee Andrea Pastorello for indepth comments on the manuscript. This work has been carried out under the INSA (Indian National Science Academy) - JSPS (Japan Society for Promotion of Science) exchange programme, and

has also been supported in part by World Premier International Research Center Initiative (WPI Initiative), MEXT, Japan, and by the Grant-in-Aid for Scientific Research of the JSPS (18104003, 18540231, 20244035, 20540226) and MEXT (19047004, 20040004).

REFERENCES

- Almog, Y., Netzer, H., 1989, MNRAS, 238, 57
 Arkharov, A., Effinova, N., Leoni, R., Di Paola, A., Di Carlo, E., Dolci, M. 2006, ATEL, 961, 1
 Benetti, S., et al. 2006, CBET, 674, 2
 Branch, D. et al. 2002, ApJ, 566, 1005
 Brown, P., Immler, S., Modjaz, M. 2006, ATEL, 916, 1
 Chevalier, R. A. 1982, ApJ, 259, 302
 Chugai, N.N., et al. 2004, MNRAS, 352, 1213
 Chugai, N., Danziger, I.J. 1994, MNRAS, 268, 173
 Clayton, D. D., 1979, Ap&SS, 65, 179
 Clocchiatti, A. et al. 2001, ApJ, 553, 886
 Crotts, A., Eastman, J., Depoy, D., Prieto, J.L., Garnavich, P. 2006, CBET 672
 Di Carlo, E. et al. 2008, ApJ, 684, 471
 Elmhamdi, A., Danziger, I. J., Cappellaro, E., Della Valle, M., Gouiffes, C., Phillips, M. M., Turatto, M. 2004, A&A, 426, 963
 Fassia, A., et al. 2000, MNRAS, 318, 1093
 Fesen, R., Milisavljevic, D., Rudie, G. 2006, CBET 672, 2
 Fransson, C. et al. 2002, ApJ, 572, 350
 Filippenko, A.V. 1997, ARA&A, 35, 309
 Filippenko, A.V., Chornock, R., 2002, IAU Circ., 7825, 1
 Foley, R.J., Smith, N., Ganeshalingam, M., Li, W., Chornock, R., Filippenko, A.V. 2007, ApJ, L105
 Gehrz, R.D. 1988, ARA&A, 26, 377
 Immler, S., et al. 2008, ApJ, 674, L85
 Landolt, A.U., 1992, AJ, 104, 340
 Martin, P., Li, W.D., Qiu, Y.L., West, D. 2002, IAU Circ., 7809, 3
 Matheson, T., Filippenko, A.V., Chornock, R., Leonard, D.C., Li, W. 2000, AJ, 119, 2303
 Matheson, T., Filippenko, A.V., Li, W., Leonard, D.C., Shields, J.C. 2001, AJ, 121, 1648
 Mattila, S., et al. 2008, MNRAS, 389, 141
 Minezaki, T., Yoshii, Y., Nomoto, K. 2007, IAU Circ., 8833, 3
 Nakano, S., Itagaki, K., Puckett, T., Gorelli, R. 2006, CBET, 666, 1
 Nozawa, T. et al. 2008, ApJ, 684, 1343
 Pastorello, A., et al. 2002, MNRAS, 333, 27
 Pastorello, A., et al. 2007, Nature, 447, 829
 Pastorello, A., et al. 2008, MNRAS, 389, 131
 Rigon, L. et al. 2003, MNRAS, 340, 191
 Richmond et al. 1996, AJ, 111, 327
 Sakon, I. et al. 2008, ApJ, in press (arXiv:0711.4801)
 Salamanca, I., Terlevich, R.J., Tenorio-Tagle, G. 2002, MNRAS, 330, 844
 Schlegel, D.J. 1990, MNRAS, 244, 269
 Smith, N., Foley, R.J., Filippenko, A.V. 2008, ApJ, 680, 568
 Soderberg, A. 2006, ATel, 917, 1
 Stritzinger, M., et al. 2002, AJ, 124, 2100
 Tominaga, N. et al. 2008, ApJ, in press (arXiv:0711.4782)